J Nanopart Res (2012) 14:748
DOI 10.1007/s11051-012-0748-1

RESEARCH PAPER

Hierarchical plasmonic-metal/semiconductor micro/nanostructures: green synthesis and application in catalytic reduction of *p*-nitrophenol

Shuyan Gao · Xiaoxia Jia · Zhengdao Li · Yanli Chen

Received: 11 September 2011 / Accepted: 17 January 2012 / Published online: 9 February 2012

Abstract Hierarchical micro/nano arrays can offer both the advantages of nano-sized building blocks and micro- or submicrometer-sized ordered arrays, therefore representing one kind of potential functional materials and having received enormous attention for a wealth of applications. In this study, four-dimensionally flower-like CuO micro/nanostructures decorated by Au nanoparticles are synthesized via an environmentally friendly route assisted by polyethylene glycol. Experiments reveal that the product demonstrates high catalytic performance for the reduction of 4-nitrophenol using $NaBH_4$ as the reducing agent, which could be attributed to the rich Au/CuO interfaces in the samples. Compared to the pure noble metal catalysts, the obtained sample is quite economic. In terms of methodology and cost-effectiveness, this study proposes an economically useful and green method to produce a highly efficient metal-based catalyst. It is also a good example for the organic combination of green chemistry and functional materials.

Keywords Catalytic activity · Green chemistry · Hierarchical micro/nano-structures · Plasmonic-metal/semiconductor heterostructure

Introduction

With the steady and fast growing field of nanoscience and nanotechnology, much attention has been focused on catalysis by metal nanoparticles (MNPs) (Nie and Emory 1997; Alayoglu et al. 2008; Larsson et al. 2009; Nishihata et al. 2002; Schrinner et al. 2009) in that they exhibit very high activity under mild conditions due to their high surface area-to-volume ratios and unique electronic and surface properties (Astruc et al. 2005; Heiz and Landman 2007; Astruc 2008; Pachon and Rothenberg 2008; Shiju and Guliants 2009; Zhang et al. 2011; Ballarin et al. 2010). Thus, significant progress has been made with regard to the design, synthesis, and utilization of MNPs (Bruchez et al. 1998; Ghosh and Pal 2007; Lee et al. 2008; Hirsch et al. 2003). In general, although MNPs with smaller size show greater catalytic activity, they tend to be less stable and prone to aggregation to minimize their surface area due to their higher surface energy, resulting in a remarkable reduction in their catalytic activities. In order to overcome this problem, MNPs are usually immobilized on less-expensive supporting materials (such as metal oxides and polymeric structures) (Esumi et al. 2004; Lu et al. 2006; Mori et al. 2004; Wang et al. 2005; Zhang et al. 2009a, b), which

Electronic supplementary material The online version of this article (doi:10.1007/s11051-012-0748-1) contains supplementary material, which is available to authorized users.

S. Gao (✉) · X. Jia · Z. Li · Y. Chen
College of Chemistry and Environmental Science, Henan Normal University, 46 Jianshe Street, Xinxiang 453007, Henan, People's Republic of China
e-mail: shuyangao@htu.cn

also facilitates catalyst recycling (Astruc et al. 2005; Rao et al. 2002; Ishida and Haruta 2007). For example, heterogeneous catalysts containing noble metals, such as Ag, Pd, Pt, and Au have been successfully deposited onto metal oxide supports via the wetness impregnation method or the deposition–precipitation method (Arve et al. 2006; Zhang et al. 2009a, b; Delannoy et al. 2006). As an alternative, hierarchical micro/nanostructures with well-defined morphologies have progressively attracted considerable attention in this field because the physicochemical nature of their organic/inorganic components and the synergy between these components endow them with higher functionality and performance (Fang et al. 2008; Gao et al. 2011a, b, c; Li et al. 2009, 2011).

As well-documented, aminoaromatics like 4-aminophenol (4-AP) are very useful in a wealth of applications that include analgesic and antipyretic drugs, photographic developer, corrosion inhibitor, anticorrosion-lubricant, and so on (Du et al. 2004; Corbett 1999; Rode et al. 1999). The reduction of 4-nitrophenol (4-NP) over MNPs in the presence of sodium borohydride ($NaBH_4$) has been rigorously investigated for the efficient production of 4-AP (Zhang et al. 2011; Deng et al. 2010; Jiang, et al. 2011; Sarkar et al. 2011; Liu and Zhao 2009; Huang et al. 2009; Zhu et al. 2011). Such transformation reaction has been in turn used as a model to test the catalytic activity of different MNPs like single MNPs (Zhang et al. 2011), bimetallic nanostructures (Zhu et al. 2011), and core–shell MNPs (Jiang et al. 2011; Mei et al. 2007), due to the simple procedure and easily available equipment (Ballarin et al. 2010; Dotzauer et al. 2009; Kuroda et al. 2009). In this field, the research for alternative MNPs-based catalytic materials via immobilization of MNPs on cheap supporting materials or formation of hierarchical micro/nanostructures through facile and green routes is pressing.

The environmentally friendly synthesis has been well documented in fabricating inorganic materials due to its green concept. Recently, we have developed a simple and green method for generating a series of hierarchical micro/nanostructures with great potentials in a range of electrical, optical, and biomedical applications (Gao et al. 2005, 2006a, b, 2008a, b, 2010a, b, c, 2011a, b, c; Lu et al. 2008a, b). Herein, an environment-friendly polyethylene glycol (PEG)-assisted hydrothermal strategy has been successfully furthered for the synthesis of three-dimensionally (3D) hierarchical Au/CuO micro/nanostructures, which were constructed from self-assembling of 1D nanosheets. The as-prepared samples were tested to catalyze the reduction of 4-NP with an excess amount of $NaBH_4$. Especially, to have an in-depth understanding of the catalytic mechanism of this heterostructure, the influence of different contents of Au on the catalytic performance has been emphasized. The experimental results show that there are several factors affecting the catalytic activities of micro/nanostructured Au/CuO samples, including the size of the AuNPs, the content of the AuNPs, and the interface number between the Au and CuO.

Experimental

Chemicals and materials

All chemical reagents were of analytical grade and used without further purification. All water used in this investigation was deionized by a Nanopure filtration system to a resistivity of 18 MΩ cm.

Green synthesis of hierarchical Au/CuO micro/nanostructures

The preparation of PEG-assisted synthesis of hierarchical Au/CuO micro/nanostructures is straightforward. In a typical procedure, an aqueous solution (30 mL) containing cupric sulfate (0.025 M), certain amount of 0.0254 M aqueous solution of chloroauric acid, and a PEG solution (10 mL, 0.03 M) were mixed with agitation in a beaker. Then, the blue solution was formed after an aqueous ammonia solution (1 mL, 28 wt%) was added dropwise to the above mixture. The mixture was then transferred into a stainless steel autoclave with a Teflon liner of 50 mL capacity, and heated in an oven at 403 K for 4 h. After the autoclave was air-cooled to room temperature unaided, a large quantity of black precipitate and a colorless supernatant were obtained. The resulting black precipitate was filtered and washed with distilled water, and finally dried in air naturally.

Sample characterizations

The crystallinity and the effect of Au modification in the crystal phases of the synthesized CuO were

characterized by the X-ray diffraction (XRD) technique with a Ragaku-D/Max 2500 V/PC X-ray diffractometer in the diffraction angle range $2\theta = 25$–$70°$, using Cu Kα radiation at 40 kV and 200 mA. The morphologies of the as-prepared samples were observed by the field emission scanning electron microscopy (FESEM) on an XL30 ESEM FEG scanning electron microscopy operating at 20 kV. The attached the energy dispersive X-ray (EDX) probe allowed microscopic elemental analysis of the sample under FESEM. Microstructure analysis was carried out by the high resolution transmission electron microscopy (HRTEM), taken with a JEOL JEM-2010 transmission electron microscope. The surface property of all as-prepared samples was determined by the X-ray photoelectron spectroscopy (XPS), which was collected on an ESCALab MKII X-ray photoelectron spectrometer, using non-monochromatized Mg Kα X-ray as excitation source.

Tests on the catalytic activity of the sample

The catalytic hydride reduction of 4-NP to 4-AP with an excess amount of $NaBH_4$ (Eq. 1) has often been used as a model to examine the catalytic performance of MNPs due to the simple procedure and easily available equipment. Herein, the as-prepared samples were tested to catalyze the reduction of 4-NP with an excess amount of $NaBH_4$. In a typical catalytic reaction, 0.0038 g $NaBH_4$ powder and 3.05 mL ultrapure water were added to 50 μL of aqueous 4-NP solution (0.005 M) in a quartz cuvette at 275 K, followed by the addition of 0.08 mg of catalyst, and the mixture was quickly subjected to UV–Vis measurements (Beijing Purkinje General Instrument Co., Ltd.). The initially obtained data can be designated as the start for the reaction time, $t = 0$. Afterward, the solution was measured every 2.5 min to track the reaction. Actually, as the reaction proceeds, one could observe the gradual change of the solution color from yellow to colorless.

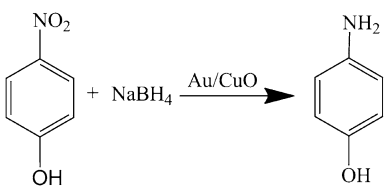

1

Results and discussion

Morphology analyses

In order to obtain detailed information about the microstructure and morphology of the as-synthesized samples, the FESEM observations are carried out and shown in Fig. 1. The low magnified image (Fig. 1a) indicates that the panoramic morphology of the as-prepared sample is hierarchically flower-like with a diameter ranging from 2 to 3.5 μm. The clear view (Fig. 1c, d) displays that the surface of the architecture is not smooth and consists of many nanosheets with average thickness of ca. 30 nm. Thus, the product is named as 3D hierarchical micro/nanostructures. Here, besides functioning as a reducing agent, PEG is also a capping agent. The dominant morphology of CuO was mat composed of interconnected nanosheets in the absence of any capping agent (Gao et al. 2008a, b).

Figure 2a gives the elemental spectrum of the Au/CuO micro/nanostructure revealed by EDX analysis. It indicates that the Au/CuO hierarchical structure is only composed of three elements, Au, Cu, and O. Figure 2b gives the HRTEM image of the interface structures between Au and CuO crystals. The plane fringe with a 2.08 Å crystalline plane spacing is assigned to the Au (200) planes, and the size of Au particle is about 3 nm. The spacing between adjacent lattice fringes is 2.56 Å, which is close to the *d* spacing of the (002) plane of CuO. These indicate that Au nanoparticles are on the CuO surface, not incorporating into the lattice of CuO. The mean sizes of Au/CuO micro/nanostructures with different Au contents were determined by HRTEM images to be about 1.8, 5, 8, and 12 nm, respectively, as shown in Figure S1 in Electronic Supplementary Material.

XRD characterizations

The XRD patterns of the as-synthesized Au/CuO samples with different Au contents are shown in Fig. 3. All curves in Fig. 3 can be well indexed to the monoclinic symmetry of CuO (space group *C*2/*c*, $a = 4.684$ Å, $b = 3.425$ Å, $c = 5.129$ Å, $\beta = 99.47°$, JCPDS File No. 05-0661) and metallic Au. The intensity of CuO reflection peaks is much stronger than that of Au because of the low content of Au in all the samples. No characteristic peaks of impurities and other phases such as $Cu(OH)_2$ and Au_2O_3 are observed. In

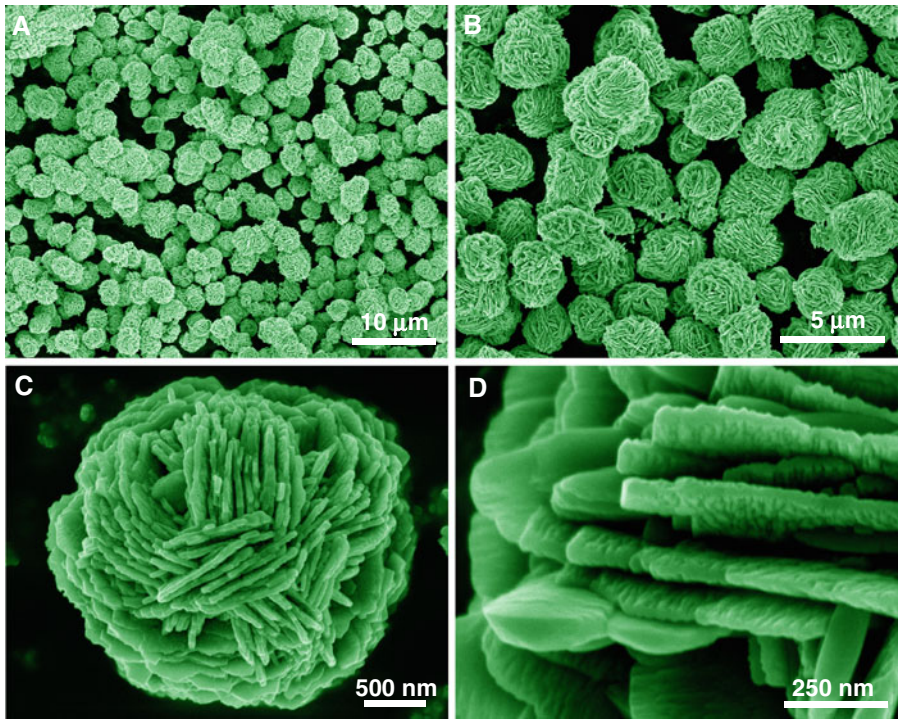

Fig. 1 FESEM images of the as-prepared samples: **a** a low-magnification panoramic view of hierarchical Au/CuO micro/nanostructures with Au content of 0.36 at.% in the presence of PEG; **b** a high-magnification image of (**a**); **c** a single microflower; and **d** the surface of the microflower

addition, there is no remarkable shift of all diffraction peaks and lattice parameters of CuO in all Au/CuO samples compared to that of pure CuO, suggesting that Au does not incorporate into the lattice of CuO, but as metal deposit on the surface. These data demonstrate that PEG successfully reduced the Au(III) to Au (0) under the present hydrothermal condition. A Cu–O–Au bond may be formed between metallic Au and CuO nanocrystals, leading to the formation of Au/CuO metal/semiconductor micro/nanostructures assembling from the nano-scaled blocks via PEG.

Surface structure of hierarchical Au/CuO micro/nanostructures

The surface components and chemical states of the as-prepared sample with Au content of 0.36 at.% are investigated by XPS analysis, and the corresponding results are shown in Fig. 4. The peaks originating from Cu, Au, O, and C elements are clearly discerned. The presence of C comes mainly from pump oil due to vacuum treatment before the XPS test. Figure 4b–d displays the high-resolution spectra for O, Cu, and Au species, respectively. In Fig. 4c, the Cu 2p3/2 fine spectrum reveals a main peak at 933.7 eV, which is accompanied by two satellite peaks at 941.1 and 943.1 eV, respectively. These features correspond to a Cu^{2+} state for Cu atoms, which are well consistent with those observed in CuO (Gao et al. 2011a, b, c; Cao et al. 2007). Moreover it can be seen that the peak positions of Cu 2p3/2 in CuO and Au/CuO samples are nearly at the same value, confirming that the Cu element exists mainly in the form of Cu^{2+} on both sample surfaces (Gao et al. 2011a, b, c). Figure 4d shows the Au 4f XPS spectrum for the sample. The Au 4f7/2 peak appears at a binding energy of 84.0 eV, and the splitting span of the 4f doublet is 3.6 eV, indicating the metallic nature of Au (Gao et al. 2009, 2010a, b, c).

Catalytic test

Catalytic performance of hierarchical Au/CuO micro/nanostructures in 4-NP reduction

As we know, aminoaromatics like 4-AP are significant intermediates for different industrial products, and

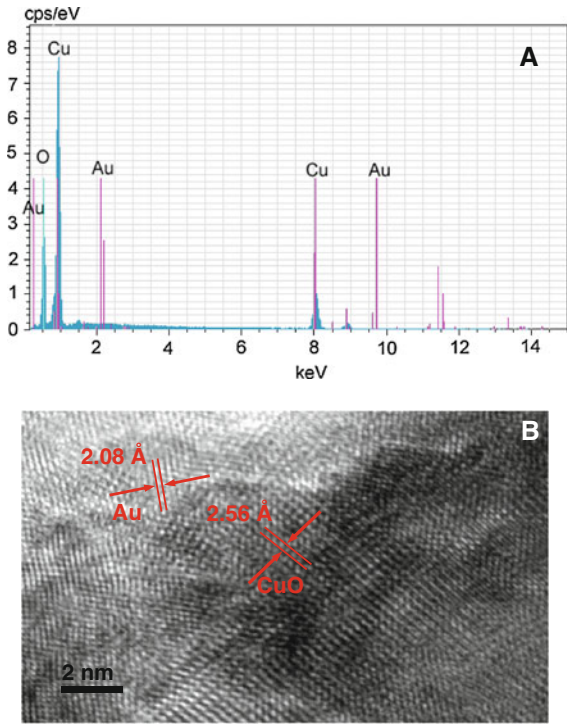

Fig. 2 **a** A random EDX spectrum of the sample; **b** HRTEM image of the product

therefore a number of catalytic methods for reduction of nitroaromatics have been used to accomplish this transformation. Therefore, we used the reduction of 4-NP to 4-AP with an excess amount of $NaBH_4$ as a model system to quantitatively evaluate the catalytic activity of the obtained hierarchical Au/CuO micro/nanostructures. As shown in Figs. 5a, 4-NP solution exhibits a strong absorption peak at 317 nm in neutral or acidic conditions which when treated with an aqueous solution of $NaBH_4$ is remarkably red-shifted to 400 nm. This is because of the formation of 4-nitrophenolate ions owing to an increase in solution alkalinity upon the addition of $NaBH_4$ (Praharaj et al. 2004). The reaction was kinetically inert at this stage and could proceed after the catalyst of hierarchical Au/CuO micro/nanostructures was added. The kinetics could be easily monitored spectrophotometrically associated with its perceptible color change with the fading and ultimate bleaching of the yellow color of the 4-NP solution and a concomitant appearance of a new peak at $\sim$302 nm, addressing the formation of 4-AP (Fig. 5a) (Sarkar et al. 2011). Noteworthily, the reaction does not start immediately after the addition of the catalyst, but only after a noticeable time lag

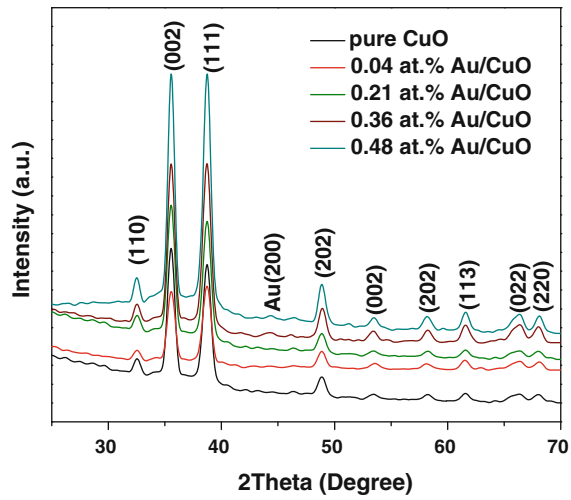

Fig. 3 XRD patterns of the Au/CuO samples with various gold contents

(Fig. 5b, t_0), i.e., induction time (IT). This may be ascribed to that $NaBH_4$ has to be first decomposed on the surface of nanoparticles, producing H-atoms, which are then available to 4-NP molecules (Khalavka et al. 2009). Once the reduction starts, the plot of $\ln(A/A_0)$ *versus* time displays a linear correlation, as shown in Fig. 5b. Because an excess of $NaBH_4$ was used, the first approximation was to fit the kinetic data with a first-order rate law (Mei et al. 2005; 2007; Panigrahi et al. 2007). The apparent rate constant k_a defined through Eq. 2, which was obtained from the linear slope, was analyzed to be 0.10176 min^{-1} at 275 K under the reaction condition as shown in Fig. 5.

$$\frac{dc_{4-NP}}{dt} = -k_a c_{4-NP} \tag{2}$$

Effects of Au contents on 4-NP reduction

To study the effect of the catalyst concentration on the rate of reduction, four different Au contents, i.e., 0 at.%, 0.04 at.%, 0.21 at.%, 0.36 at.%, 0.48 at.%, 100 at.% were used. The amounts of Au in the sample are actual content in the catalysts, which were tested by XPS. The decreases in the absorbance at 400 nm are shown in Fig. 6. With 0 at.% Au, the concentration of 4-NP is rarely changed within 120 min. With 0.04 at.% Au, the complete reduction was achieved within 80 min. With 0.21, 0.36, and 0.48 at.% Au, the reaction was completed within 32.5, 15, and 17.5 min, respectively. From Fig. 7, the apparent reaction rates

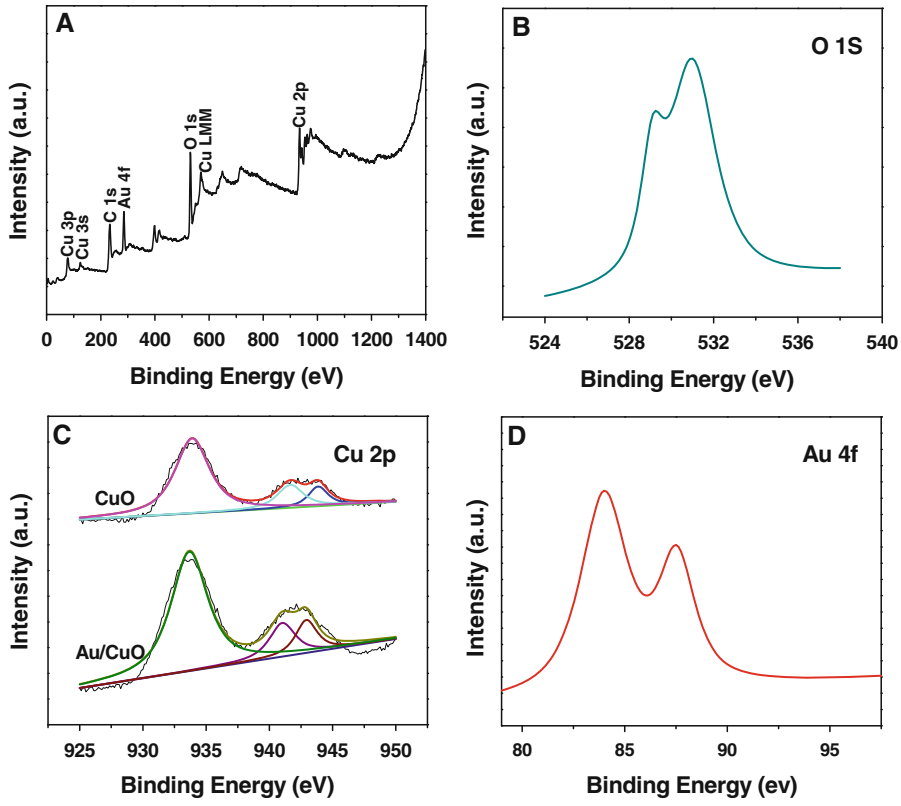

Fig. 4 XPS spectra of the as-synthesized sample with Au content of 0.36 at.%: **a** XPS full spectrum of the sample; **b** O 1 s spectrum; **c** Cu 2p3/2 spectrum; and **d** Au 4f spectrum

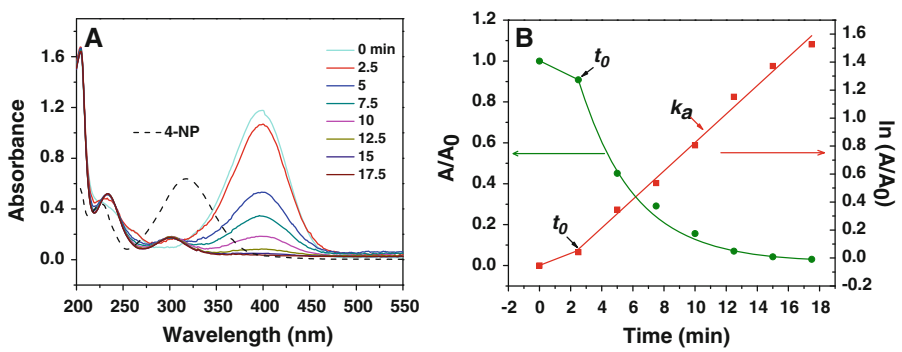

Fig. 5 **a** UV–Vis absorption spectra during the catalytic reduction of 4-NP over hierarchical Au/CuO micro/nanostructures with Au content of 0.36 at.%; **b** the *blue* and *red curves* were the A/A_o and $\ln(A/A_o)$ versus reaction time for the reduction of 4-NP over hierarchical Au/CuO micro/nanostructures, respectively. A_o and A was the absorption peak at 400 nm initially and at time t. The induction period t_0 is marked with the *black arrow*. Condition: [4-NP], 0.80×10^{-4} M; $[NaBH_4]$, 3.24×10^{-2} M; Au/CuO, 0.08 mg. T, 275 K

were calculated to be 0.00131, 0.01652, 0.04431, 0.10176, 0.07855, and 0.00047 min^{-1} for the six different catalysts with Au contents, 0 at.%, 0.04 at.%, 0.21 at.%, 0.36 at.%, 0.48 at.%, and 100 at.%, respectively. The result demonstrates that the increase in the Au content significantly enhanced the 4-NP reduction initially. However, there is an optimal Au content in the catalytic activity, i.e., 0.36 at.%. Also, the Au/CuO micro/nanostructures are superior catalysts than Au itself, presumably attributed to the electronic junction effect of Au and CuO (Lee et al. 2010; Lopes et al. 2010; Costi et al. 2010; Lin and Doong 2011). In fact, pure gold is generally not catalytic unless it is in the form of small NPs (<5 nm),

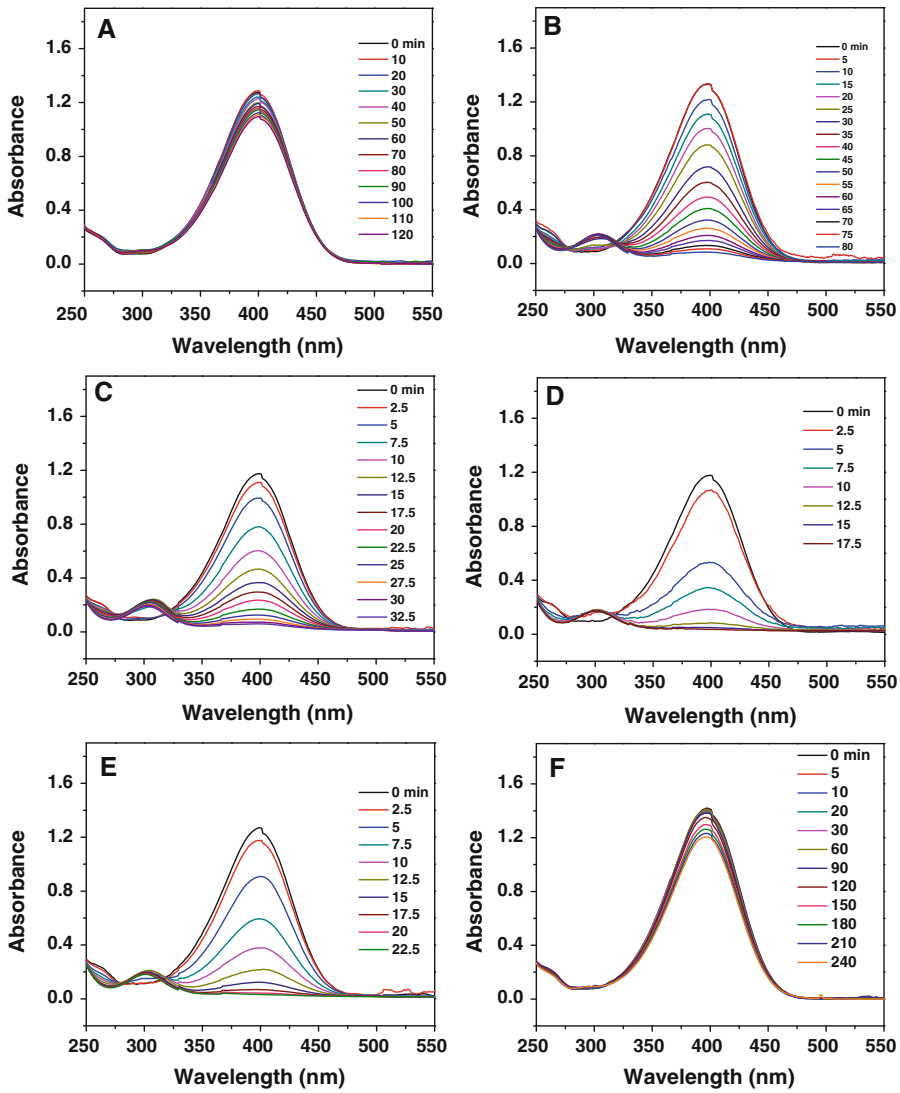

Fig. 6 UV–Vis spectra of 4-NP in the presence of Au/CuO with different Au contents. **a** 0 at.%; **b** 0.04 at.%; **c** 0.21 at.%; **d** 0.36 at.%; **e** 0.48 at.%; and **f** 100 at.%. The reaction conditions are the same as shown in Fig. 5

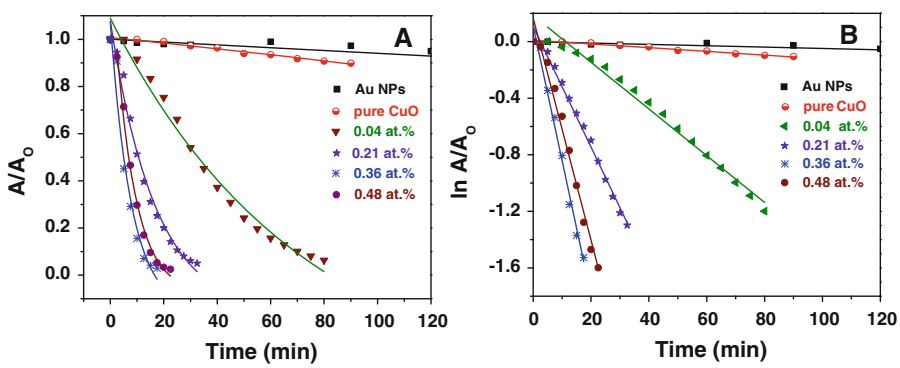

Fig. 7 **a**, **b** are plots of A/A_o and ln (A/A_o) versus time, respectively, for the reduction of 4-NP corresponding to the data and reaction conditions are the same as shown in Fig. 5

in combination with other metals, or as cations (Haruta et al. 1987; Bond and Thompson 1999; Sinfelt 1983; Fu et al. 2003; Hutchings 2002; Nutt et al. 2005).

In order to judge our catalytic results via comparison with the reported ones about the reduction of 4-NP, we measured the apparent rate constant to be

Table 1 Comparison of the catalytic activity of the obtained Au/CuO micro/nanostructures with Au content of 0.36 at.% for the reduction of 4-NP with AuNPs reported in the literature

Catalysts	T/K	[Au] $\times 10^5$/M	[4-NP] $\times 10^4$/M	[$NaBH_4$] $\times 10^2$/M	ka $\times 10^3/s^{-1}$
Au (Zhang et al. 2011)	298	3.0	0.6	0.25	10.64
Au/Ag (Huang et al. 2009)	298	74	0.66	1.0	6.07
Au (Zhu et al. 2011)	298	1.5	1.61	6.45	5.67
Au (Ballarin et al. 2010)	295	0.35	0.52	8.3	7.0
Au@Ag (Jiang et al. 2011)	298	1.34	1.03	16.3	4.97
Our sample	298	0.2	0.81	3.24	15.94

0.01594 s^{-1} in the presence of 0.06 mg Au/CuO micro/nanostructures with Au content of 0.36 at.% at T = 298 K, as shown in Figure S2. Table 1 summarizes the data to compare the catalytic performance of our samples with those reported on Au nanoparticles. The catalytic performance in our case is smaller than that of the SPB-supported Pd (Lu et al. 2007) and SPB-supported Pt (Mei et al. 2005), and higher than that of small gold nanoparticles (Zhang et al. 2011) dendritic Ag/Au bimetallic nanostructures (Huang et al. 2009), multifunctional magnetic composite Fe_3O_4@SiO_2-LBL-Au(0) microspheres (Zhu et al. 2011), gold nanoparticle-containing membranes (Ballarin et al. 2010), and the core–shell-structured Au@Ag catalyst under similar reaction conditions (Jiang et al. 2011). Considering the much lower content of Au in our sample and the facile and green preparation procedure, we propose an economically useful and green method to produce a highly efficient and cost-effective MNPs-based catalyst.

Reasons behind the catalytic performance of hierarchical Au/CuO micro/nanostructures

In the case of the reduction of solvated 4-NP by BH_4^-, the kinetic barrier between the two negative ions is too high for the reaction to proceed. The presence of a catalyst (e.g., MNPs) is important for this redox reaction. Donors like the BH_4^- ions supply electrons to the catalyst and thereby allow the 4-NP absorbed on the catalyst to take electrons (Zhu et al. 2011). With respect to the higher catalytic activity exhibited by Au/CuO plasmonic-metal–semiconductor composite, this may be mainly related to the number of Au/CuO interfaces. It is known that the work function of CuO and Au are 5.3 and 5.1 eV, respectively. Au has a lower work function than CuO. Therefore, electrons leave the Au from a depleted region near an Au/CuO interface into CuO, which ends up with a lacking-electron region (see Scheme 1, region D) and surplus-electrons region (region E). The existence of these regions facilitates the diffusion of charged 4-nitrophenolate ions on the catalyst surface and the consequent uptake of electrons by 4-nitrophenolate ions that happen to be close to (on top of) these regions. From Figure S1, it can be seen that large AuNPs provide large surface areas, in turn increase the interface area (Lee et al. 2010). If the AuNPs are too large, however, the number of AuNPs is decreased, so the number of accessible interfaces is bound to decrease, which will not facilitate the catalytic performance. The more interfaces there are, the more such regions exist. This in turn increases the chances for randomly absorbed 4-NP to happen to be on top of such regions. Of course, the more interfaces exclusively facilitates the catalytic reaction.

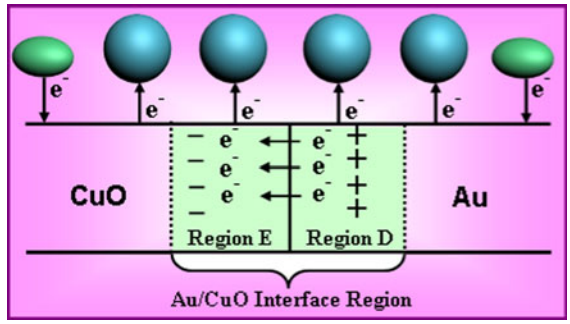

Scheme 1 Diagram of the Au/CuO interface for Au/CuO micro/nanostructures. The *green* oblate spheres stand for BH_4^-, and *blue* spheres for 4-nitrophenolate ions

Conclusions

In conclusion, hierarchical Au/CuO micro/nanostructures have been successfully synthesized through a

friendly hydrothermal method. Here, PEG successfully reduced the Au(III) to Au (0) under the present hydrothermal condition. A Cu–O–Au bond may be formed between metallic Au and CuO nanocrystals, leading to the formation of Au/CuO metal/semiconductor micro/nanostructures assembling from the nanoscaled blocks via PEG. Compared to the pure metallic catalysts, our sample shows high catalytic performance for the reduction of 4-NP to 4-AP. It is speculated that, several factors can affect the catalytic activities of micro/nanostructured Au/CuO samples. First, the larger AuNPs offer higher activity due to the larger interconnection area between Au and CuO. Second, the content of the AuNPs influences the catalytic activity. As the Au content increases, catalytic performance is improved, eventually attaining the optimal activity at Au content of 0.36 at.% and then lessening. Third, The more interfaces there are, the more such regions exist. This in turn increases the chances for randomly absorbed 4-NP to happen to be on top of such regions, therefore exclusively facilitating the catalytic reaction.

Acknowledgments The authors are grateful to the editor and referees for their constructive comments and suggestions. This study was supported by the National Natural Science Foundation of China (21071047), Program for New Century Excellent Talents in University (NCET), the Project Sponsored by the Scientific Research Foundation for the Returned Overseas Chinese Scholars, State Education Ministry of China, Excellent Youth Foundation of He'nan Scientific Committee, and the Program for Science & Technology Innovation Talents in Universities of Henan Province (2011HASTIT010).

References

Alayoglu S, Nilekar AU, Mavrikakis M, Eichhorn B (2008) Ru–Pt core-shell nanoparticles for preferential oxidation of carbon monoxide in hydrogen. Nat Mater 7:333–338

Arve K, Svennerberg K, Klingstedt F, Eranen K, Wallenberg LR, Bovin JO, Capek L, Murzin DY (2006) Structure-activity relationship in HC-SCR of NOx by TEM, O_2-chemisorption, and EDXS study of Ag/Al_2O_3. J Phys Chem B 110:420–427

Astruc D (2008) Nanoparticles and catalysis. Wiley, Weinheim

Astruc D, Lu F, Aranzaes JR (2005) Nanoparticles as recyclable catalysts: the frontier between homogeneous and heterogeneous catalysis. Angew Chem Int Ed 44:7852–7872

Ballarin B, Cassani MC, Tonelli D, Boanini E, Albonetti S, Blosi M, Gazzano M (2010) Gold nanoparticle-containing membranes from in situ reduction of a gold(III)-aminoethylimidazolium aurate salt. J Phys Chem C 114:9693–9701

Bond GC, Thompson DT (1999) Catalysis by gold. Catal Rev Sci Eng 41:319–388

Bruchez M, Moronne M, Gin P, Weiss S, Alivisatos AP (1998) Semiconductor nanocrystals as fluorescent biological labels. Science 281:2013–2016

Cao A, Monnell JD, Matranga C, Wu J, Cao L, Gao D (2007) Hierarchical nanostructured copper oxide and its application in arsenic removal. J Phys Chem C 111:18624–18628

Corbett JF (1999) An historical review of the use of dye precursors in the formulation of commercial oxidation hair dyes. Dyes Pigm 41:127–136

Costi R, Saunders AE, Banin U (2010) Colloidal hybrid nanostructures: a new type of functional materials. Angew Chem Int Ed 49:4878–4897

Delannoy L, El Hassan N, Musi A, Le To NN, Krafft JM, Louis C (2006) Preparation of supported gold nanoparticles by a modified incipient wetness impregnation method. J Phys Chem B 110:22471–22478

Deng Y, Cai Y, Sun Z, Liu J, Liu C, Wei J, Li W, Liu C, Wang Y, Zhao D (2010) Multifunctional mesoporous composite microspheres with well-designed nanostructure: a highly integrated catalyst system. J Am Chem Soc 132:8466–8473

Dotzauer DM, Bhattacharjee S, Wen Y, Bruening ML (2009) Nanoparticle-containing membranes for the catalytic reduction of nitroaromatic compounds. Langmuir 25: 1865–1871

Du Y, Chen H, Chen R, Xu N (2004) Synthesis of p-aminophenol from *p*-nitrophenol over nano-sized nickel catalysts. Appl Catal A 277:259–264

Esumi K, Isono R, Yoshimura T (2004) Preparation of PAMAM- and PPI-metal (silver, platinum, and palladium) nanocomposites and their catalytic activities for reduction of 4-nitrophenol. Langmuir 20:237–243

Fang XS, Bando Y, Gautam UK, Ye CH, Golberg DJ (2008) Inorganic semiconductor nanostructures and their field-emission applications. Mater Chem 18:509–522

Fu Q, Saltsburg H, Flytzani-Stephanopoulos M (2003) Active nonmetallic Au and Pt species on ceria-based water-gas shift catalysts. Science 301:935–938

Gao S, Zhang H, Wang X, Yang J, Zhou L, Peng C, Sun D, Li M (2005) Unique gold sponges: biopolymer-assisted hydrothermal synthesis and potential application as surface-enhanced Raman scattering substrates. Nanotechnology 16:2530–2535

Gao S, Zhang H, Deng R, Wang X, Sun D, Zheng G (2006a) Engineering white light-emitting Eu-doped ZnO urchins by biopolymer-assisted hydrothermal method. Appl Phys Lett 89:123125-1–123125-3

Gao S, Zhang H, Wang X, Deng R, Sun D, Zheng G (2006b) ZnO-based hollow microspheres: biopolymer-assisted assemblies from ZnO nanorods. J Phys Chem B 110: 15847–15852

Gao S, Yang S, Shu J, Zhang S, Li Z, Jiang K (2008a) Green fabrication of hierarchical CuO hollow micro/nanostructures and enhanced performance as electrode materials for lithium-ion batteries. J Phys Chem C 112:19324–19328

Gao S, Zhang S, Jiang K, Yang S, Lu W (2008b) Biopolymer-assisted synthesis of single crystalline gold disks by a hydrothermal route. Curr Nanosci 4:145–150

Gao S, Koshizaki N, Koyama E, Tokuhisa H, Sasaki T, Kim J-K, Cho Y, Kim D-S, Shimizu Y (2009) Innovative platform for transmission localized surface plasmon transducers and its application in detecting heavy metal Pd(II). Anal Chem 81:7703–7712

Gao S, Koshizaki N, Tokuhisa H, Koyama E, Sasaki T, Kim J-K, Ryu Y, Kim D-S, Shimizu Y (2010a) Highly stable Au nanoparticles with tunable spacing and their potential application in surface plasmon resonance biosensors. Adv Funct Mater 20:78–86

Gao S, Li Z, Jia X, Jiang K, Zeng H (2010b) Bioinspired synthesis of well faceted CuI nanostructures and evaluation of their catalytic performance for coupling reactions. Green Chem 12:1442–1447

Gao S, Li Z, Zhang H (2010c) Bioinspired green synthesis of nanomaterials and their applications. Curr Nanosci 6:452–468

Gao S, Jia X, Li Z, Chen Y, Jiang K (2011a) Antibiotic-inspired zinc oxide with morphology-dependent photocatalytic activity. Can J Chem 89:590–597

Gao S, Jia X, Yang S, Li Z, Jiang K (2011b) Hierarchical Ag/ZnO micro/nanostructure: green synthesis and enhanced photocatalytic performance. J Solid State Chem 184:764–769

Gao S, Li Z, Jiang K, Zeng H, Li L, Fang X, Jia X, Chen Y (2011c) Biomolecule-assisted in situ route toward 3D superhydrophilic Ag/CuO micro/nanostructures with excellent artificial sunlight self-cleaning performance. J Mater Chem 21:7281–7288

Ghosh SK, Pal T (2007) Interparticle coupling effect on the surface plasmon resonance of gold nanoparticles: from theory to applications. Chem Rev 107:4797–4862

Haruta M, Kobayashi T, Sano H, Yamada N (1987) Novel gold catalysts for the oxidation of carbon monoxide at a temperature far below 0 °C. Chem Lett 16:405–408

Heiz U, Landman U (2007) Nanocatalysis: nanoscience and technology. Springer, Berlin

Hirsch LR, Stafford RJ, Bankson JA, Sershen SR, Rivera B, Price RE, Hazle JD, Halas NJ, West JL (2003) Nanoshell-mediated near-infrared thermal therapy of tumors under magnetic resonance guidance. Proc Natl Acad Sci USA 100:13549–13554

Huang J, Vongehr S, Tang S, Lu H, Shen J, Meng X (2009) Ag dendrite-based Au/Ag bimetallic nanostructures with strongly enhanced catalytic activity. Langmuir 25:11890–11896

Hutchings GJ (2002) Gold catalysis in chemical processing. Catal Today 72:11–17

Ishida T, Haruta M (2007) Gold catalysts: towards sustainable chemistry. Angew Chem Int Ed 46:7154–7156

Jiang H, Akita T, Ishida T, Haruta M, Xu Q (2011) Synergistic catalysis of Au@Ag core-shell nanoparticles stabilized on metal-organic framework. J Am Chem Soc 133:1304–1306

Khalavka Y, Becker J, Sönnichsen C (2009) Synthesis of rod-shaped gold nanorattles with improved plasmon sensitivity and catalytic activity. J Am Chem Soc 131:1871–1875

Kuroda K, Ishida T, Haruta M (2009) Reduction of 4-nitrophenol to 4-aminophenol over Au nanoparticles deposited on PMMA. J Mol Catal A 298:7–11

Larsson EM, Langhammer C, Zorić I, Kasemo B (2009) Nanoplasmonic probes of catalytic reactions. Science 326:1091–1094

Lee JS, Ulmann PA, Han MS, Mirkin CA (2008) A DNA-gold nanoparticle-based colorimetric competition assay for the detection of cysteine. Nano Lett 8:529–533

Lee YM, Garcia MA, Huls NAF, Sun SH (2010) Synthetic tuning of the catalytic properties of Au-Fe_3O_4 nanoparticles. Angew Chem Int Ed 122:1293–1296

Li L, Li Y, Gao S, Koshizaki N (2009) Ordered Co_3O_4 hierarchical nanorod arrays: tunable superhydrophilicity without UV irradiation and transition to superhydrophobicity. J Mater Chem 19:8366–8371

Li Y, Koshizaki N, Cai W (2011) Periodic one-dimensional nanostructured arrays based on colloidal templates, applications, and devices. Coordin Chem Rev 255:357–373

Lin F, Doong R (2011) Bifunctional Au-Fe_3O_4 heterostructures for magnetically recyclable catalysis of nitrophenol reduction. J Phys Chem C 115:6591–6598

Liu P, Zhao MF (2009) Silver nanoparticle supported on halloysite nanotubes catalyzed reduction of 4-nitrophenol (4-NP). Appl Surf Sci 255:3989–3993

Lopes G, Vargas JM, Sharma SK, Béron F, Pirota KR, Knobel M, Rettori C, Zysler RD (2010) Ag-Fe_3O_4 dimer colloidal nanoparticles: synthesis and enhancement of magnetic properties. J Phys Chem C 114:10148–10152

Lu Y, Mei Y, Drechsler M, Ballauff M (2006) Thermosensitive core-shell particles as carriers for Ag nanoparticles: modulating the catalytic activity by a phase transition in networks. Angew Chem Int Ed 45:813–816

Lu Y, Mei Y, Schrinner M, Ballauff M, Moller MW (2007) In situ formation of Ag nanoparticles in spherical polyacrylic acid brushes by UV irradiation. J Phys Chem C 111:7676–7681

Lu W, Gao S, Wang J (2008a) One-pot synthesis of Ag/ZnO self-assembled 3D hollow microspheres with enhanced photocatalytic performance. J Phys Chem C 112:16792–16800

Lu W, Liu G, Gao S, Xing S, Wang J (2008b) Tyrosine-assisted preparation of Ag/ZnO nanocomposites with enhanced photocatalytic performance and synergistic antibacterial activities. Nanotechnology 19:445711–445721

Mei Y, Sharma G, Lu Y, Ballauff M, Drechsler M, Irrgang T, Kempe R (2005) High catalytic activity of platinum nanoparticles immobilized on spherical polyelectrolyte brushes. Langmuir 21:12229–12234

Mei Y, Lu Y, Polzer F, Ballauff M (2007) Catalytic activity of palladium nanoparticles encapsulated in spherical polyelectrolyte brushes and core-shell microgels. Chem Mater 19:1062–1069

Mori K, Hara T, Mizugaki T, Ebitani K, Kaneda K (2004) Hydroxyapatite-supported palladium nanoclusters: a highly active heterogeneous catalyst for selective oxidation of alcohols by use of molecular oxygen. J Am Chem Soc 126:10657–10666

Nie S, Emory SR (1997) Probing single molecules and single nanoparticles by surface-enhanced Raman scattering. Science 275:1102–1106

Nishihata Y, Mizuki J, Akao T, Tanaka H, Uenishi M, Kimura M, Okamoto T, Hamada N (2002) Self-regeneration of a Pd-perovskite catalyst for automotive emissions control. Nature 418:164–167

Nutt MO, Hughes JB, Wong MS (2005) Designing Pd-on-Au bimetallic nanoparticle catalysts for trichloroethene hydrodechlorination. Environ Sci Technol 39:1346–1353

Pachon LD, Rothenberg G (2008) Transition-metal nanoparticles: synthesis, stability and the leaching issue. Appl Organomet Chem 22:288–299

Panigrahi S, Basu S, Praharaj S, Pande S, Jana S, Pal A, Gosh SK, Pal T (2007) Synthesis and size-selective catalysis by supported gold nanoparticles: study on heterogeneous and homogeneous catalytic process. J Phys Chem C 111:4596–4605

Praharaj S, Nath S, Ghosh SK, Kundu S, Pal T (2004) Immobilization and recovery of Au nanoparticles from anion exchange resin: resin-bound nanoparticle matrix as a catalyst for the reduction of 4-nitrophenol. Langmuir 20:9889–9892

Rao CNR, Kulkarni GU, Thomas PJ, Edwards PP (2002) Size-dependent chemistry: properties of nanocrystals. Chem Eur J 8:28–35

Rode CV, Vaidya MJ, Chaudhari RV (1999) Synthesis of *p*-aminophenol by catalytic hydrogenation of nitrobenzene. Org Process Res Dev 3:465–470

Sarkar S, Sinha AK, Pradhan M, Basu M, Negishi Y, Pal T (2011) Redox transmetalation of prickly nickel nanowires for morphology controlled hierarchical synthesis of nickel/gold nanostructures for enhanced catalytic activity and SERS responsive functional material. J Phys Chem C 115:1659–1673

Schrinner M, Ballauff M, Talmon Y, Kauffmann Y, Thun J, Möller M, Breu J (2009) Single nanocrystals of platinum prepared by partial dissolution of Au-Pt nanoalloys. Science 323:617–620

Shiju NR, Guliants VV (2009) Recent developments in catalysis using nanostructured materials. Appl Catal A 356:1–17

Sinfelt JH (1983) Bimetallic catalysis: discoveries, concepts and applications. Wiley, New York

Wang AQ, Chang CM, Mou CY (2005) Evolution of catalytic activity of Au-Ag bimetallic nanoparticles on mesoporous support for CO oxidation. J Phys Chem B 109:18860–18867

Zhang H, Li X, Chen G (2009a) Ionic liquid-facilitated synthesis and catalytic activity of highly dispersed Ag nanoclusters supported on TiO_2. J Mater Chem 19:8223–8231

Zhang L, Zhang CB, He H (2009b) The role of silver species on Ag/Al_2O_3 catalysts for the selective catalytic oxidation of ammonia to nitrogen. J Catal 261:101–109

Zhang Z, Shao C, Zou P, Zhang P, Zhang M, Mu J, Guo Z, Li X, Wang C, Liu Y (2011) In situ assembly of well-dispersed gold nanoparticles on electrospun silica nanotubes for catalytic reduction of 4-nitrophenol. Chem Commun 47:3906–3908

Zhu Y, Shen J, Zhou K, Chen C, Yang X, Li C (2011) Multifunctional magnetic composite microspheres with in situ growth Au nanoparticles: a highly efficient catalyst system. J Phys Chem C 115:1614–1619